

How to identify zero modes for improved staggered fermions

Chiral Ward identities for Dirac eigenmodes with staggered fermions

Hwancheol Jeong^{1,*}, Seungyeob Jwa¹, Jangho Kim^{2,3}, Sunghee Kim¹, Sunkyu Lee¹, Weonjong Lee^{1,**}, Jeonghwan Pak¹, and (SWME Collaboration)

¹Lattice Gauge Theory Research Center, CTP, Department of Physics and Astronomy, Seoul National University, Seoul 08826, South Korea

²National Superconducting Cyclotron Laboratory, Michigan State University, East Lansing, Michigan 48824, USA

³Department of Physics and Astronomy, Michigan State University, East Lansing, Michigan 48824, USA

Abstract. We present results of the eigenvalue spectrum for the staggered Dirac operator obtained using a modified Lanczos algorithm. We identify zero modes and non-zero modes. We derive the chiral Ward identity derived from the conserved $U(1)_A$ symmetry, and check it numerically. This is the first step toward construction of an improved method to identify zero modes reliably with staggered fermions.

1 Introduction

It is important to identify zero modes for any physical observable sensitive to the topological charge such as quark condensates and chiral condensates [1–7]. Here, we present the first step toward an improved method to identify zero modes using the chirality measurement and the chiral Ward identities derived from the conserved $U(1)_A$ symmetry in staggered fermions.

2 Notations and definitions

Here, we adopt the notation of Ref. [8] except for the gauge links. In general, a staggered bilinear operator is defined as

$$\begin{aligned} \mathcal{O}_{S \times T}(x) &\equiv \bar{\chi}(x_A) [\gamma_S \otimes \xi_T]_{AB} \chi(x_B) \\ &= \bar{\chi}_a(x_A) \overline{(\gamma_S \otimes \xi_T)_{AB}} U(x_A, x_B)_{ab} \chi_b(x_B). \end{aligned} \quad (1)$$

Here χ is the staggered fermion field, a, b are color indices, and $x_A = 2x + A$ where A, B are hypercubic vectors with $A_\mu, B_\mu \in \{0, 1\}$.

$$\overline{(\gamma_S \otimes \xi_T)_{AB}} = \frac{1}{4} \text{Tr}(\gamma_A^\dagger \gamma_S \gamma_B \gamma_T^\dagger), \quad (2)$$

*Speaker, e-mail: sonchac@gmail.com

**e-mail: wlee@snu.ac.kr

where γ_s represents Dirac spin matrix, and ξ_T represents the 4×4 taste matrix.

$$U(x_A, x_B) \equiv \mathbb{P}_{\text{SU}(3)} \left[\sum_{p \in C} V(x_A, x_{p_1}) V(x_{p_1}, x_{p_2}) \cdots V(x_{p_n}, x_B) \right], \quad (3)$$

where $\mathbb{P}_{\text{SU}(3)}$ is the SU(3) projection, C represents a complete set of the shortest paths from x_A to x_B , and $V(x, y)$ represents HYP-smearred fat links [9, 10] for HYP staggered fermions [9], Fat7 fat links [10–13] for asqtad [14] or HISQ [15] staggered fermions, and thin gauge links for unimproved staggered fermions.

3 Eigenmodes of staggered fermions

Let D_s be Dirac operator for staggered fermions. Here we call *staggered fermions* collectively including unimproved staggered fermions and various improved staggered fermions such as HYP-smearred staggered fermions [9], asqtad staggered fermions [14], and HISQ staggered fermions [15]. Regardless of improvement methods, staggered Dirac operator D_s is anti-Hermitian: $D_s^\dagger = -D_s$. This restricts eigenvalues of staggered fermions to be purely imaginary or zero:

$$D_s |f_\lambda^s\rangle = i\lambda |f_\lambda^s\rangle, \quad (4)$$

where λ is real, and $|f_\lambda^s\rangle$ is an eigenvector corresponding to the eigenvalue $i\lambda$. The superscript s represents the staggered fermions.

In the meantime, the staggered Dirac operator anti-commutes with the operator $\Gamma_\varepsilon = [\gamma_5 \otimes \xi_5]$, the generator for the $U(1)_A$ symmetry: $\Gamma_\varepsilon D_s = -D_s \Gamma_\varepsilon$. For a given eigenvalue $i\lambda$ of D_s and its corresponding eigenvector $|f_\lambda^s\rangle$,

$$D_s \Gamma_\varepsilon |f_\lambda^s\rangle = -i\lambda \Gamma_\varepsilon |f_\lambda^s\rangle. \quad (5)$$

Hence there must exist another eigenvector $|f_{-\lambda}^s\rangle \propto \Gamma_\varepsilon |f_{+\lambda}^s\rangle$ with the eigenvalue $-i\lambda$. This insures that eigenvalues of staggered fermions must exist as \pm pair except for zero modes.

In practice, we calculate eigenvalues and eigenvectors of $D_s^\dagger D_s$ instead of D_s . The $D_s^\dagger D_s$ is a Hermitian and positive semi-definite operator. The eigenvalue equation of $D_s^\dagger D_s$ can be written by

$$D_s^\dagger D_s |g_{\lambda^2}^s\rangle = \lambda^2 |g_{\lambda^2}^s\rangle. \quad (6)$$

Eigenvalues of a Hermitian operator can be calculated faster than those of non-Hermitian operators. A positive semi-definite operator has non-negative eigenvalues such that we can restrict the range of eigenvalues to the non-negative region. In addition, the operator $D_s^\dagger D_s$ allows us to treat even sites and odd sites separately by even-odd preconditioning [16].

For each eigenvalue λ^2 of $D_s^\dagger D_s$, there exist two corresponding eigenvalues $\pm i\lambda$ of D_s . Hence, $|g_{\lambda^2}^s\rangle$ is composed of both $|f_{+\lambda}^s\rangle$ and $|f_{-\lambda}^s\rangle$. In other words,

$$|g_{\lambda^2}^s\rangle = c_1 |f_{+\lambda}^s\rangle + c_2 |f_{-\lambda}^s\rangle, \quad (7)$$

where c_1 and c_2 are complex numbers satisfying the normalization condition $|c_1|^2 + |c_2|^2 = 1$. In fact, we can obtain the eigenvectors $|f_{+\lambda}^s\rangle$ and $|f_{-\lambda}^s\rangle$ from $|g_{\lambda^2}^s\rangle$ by projection. Let us consider projection operators given by

$$P_\pm \equiv (D_s \pm i\lambda). \quad (8)$$

Note that P_+ removes $|f_{-\lambda}^s\rangle$ component, and P_- removes $|f_{+\lambda}^s\rangle$ component. Applying them to $|g_{\lambda^2}^s\rangle$,

$$|\psi_+\rangle \equiv P_+|g_{\lambda^2}^s\rangle = c_1 2i\lambda |f_{+\lambda}^s\rangle, \quad (9)$$

$$|\psi_-\rangle \equiv P_-|g_{\lambda^2}^s\rangle = -c_2 2i\lambda |f_{-\lambda}^s\rangle. \quad (10)$$

Now normalizing $|\psi_+\rangle$ and $|\psi_-\rangle$ give the eigenvectors $|f_{+\lambda}^s\rangle$ and $|f_{-\lambda}^s\rangle$:

$$|f_{\pm\lambda}^s\rangle = \frac{|\psi_{\pm}\rangle}{\sqrt{\langle\psi_{\pm}|\psi_{\pm}\rangle}}. \quad (11)$$

4 Eigenvalue spectrum with HYP staggered fermions

We use a variation of Lanczos algorithm to calculate eigenvalues and eigenvectors [17]. It is adapted to our purpose with several improvement techniques, such as the implicit restart [18] and the polynomial acceleration with Chebyshev polynomial [19]. We are interested only in small eigenvalues near zero. However, it is possible but quite slow if we try to make the eigenvalues of submatrices converge to those small eigenvalues using the typical Lanczos procedure. Hence, we need to introduce an acceleration method to speed up the convergence of Lanczos. We adopt the Chebyshev polynomial acceleration method [19] here.

parameter	value
gluon action	tree level Symanzik [20–22]
tadpole improvement	yes
β	4.6
geometry	12^4
a	0.125 fm
valence quarks	HYP staggered fermions [10, 23, 24]
N_f	$N_f = 0$ (quenched QCD)

Table 1. Simulation environment

Here, we perform our numerical study in quenched QCD in this paper. Details on our simulation and the gauge ensemble are described in Table 1. We use HYP staggered fermions [9] as valence quarks in our numerical study.

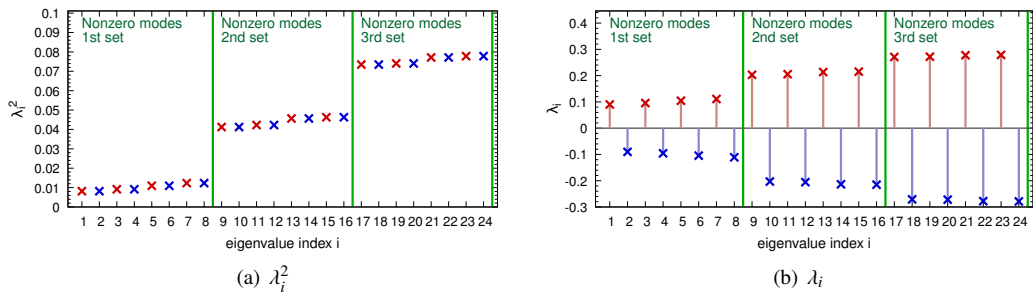


Figure 1: Eigenvalue spectrum of staggered Dirac operator on a gauge configuration with $Q = 0$. Eigenvalues are sorted by their values in ascending order.

In Fig. 1, we present the eigenvalue spectrum on a gauge configuration with topological charge $Q = 0$. Topological charge Q is determined using gauge links through the APE smearing [25]. In Fig. 1 (a), we present results of small eigenvalues λ_i^2 of the $D_s^\dagger D_s$ operator. In Fig. 1 (b), we present results of small eigenvalues λ_i of the D_s operator. Here, recall that the Lanczos algorithm produces λ_i^2 eigenvalues of $D_s^\dagger D_s$ and eigenvectors $|g_{\lambda_i^2}^s\rangle$. Using Eq. (11), we can obtain $\pm\lambda_i$ eigenvalues of D_s and eigenvectors $|f_{\pm\lambda_i}^s\rangle$. In Fig. 1 (b), we assign indices of eigenvalues such that $\lambda_{2n} = -\lambda_{2n-1}$ for $n > 0$ with $n \in \mathbb{Z}$. For each non-zero eigenvalue λ_i , we find the four-fold degeneracy near λ_i due to the approximate SU(4) taste symmetry, and for each of them there exists a $U(1)_A$ parity partner eigenmode with $\lambda = -\lambda_i$. Hence, we find an eight-fold degeneracy for each non-zero eigenmode as in Ref. [2–5].

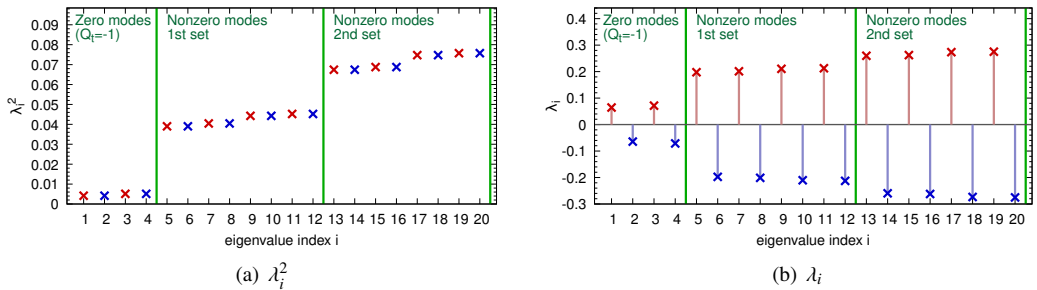


Figure 2: The same as Fig. 1 except $Q = -1$.

In Fig. 2, we present the eigenvalue spectrum on a gauge configuration with topological charge $Q = -1$. In the previous example with $Q = 0$, there is no zero mode. In case of $Q = -1$, we expect to see four-fold degenerate zero modes thanks to the approximate SU(4) taste symmetry in staggered fermions as in Refs. [2–5]. In Fig. 2, the first four eigenvalues corresponds to the would-be four-fold degenerate zero modes. They show up in pairs due to the conserved $U(1)_A$ symmetry. In other words, they satisfy $\lambda_{2n} = -\lambda_{2n-1}$: $\lambda_2 = -\lambda_1$ and $\lambda_4 = -\lambda_3$. For more details, refer to [26].

In principle, one can distinguish would-be zero modes from non-zero modes by counting the number of degenerate states: four-fold for zero modes and eight-fold for non-zero modes. However, this idea might not work well when the eigenvalue spectrum is too dense in a large volume to classify them into groups of degenerate eigenvalues. Hence, it is necessary to have a significantly improved method to identify zero modes more reliably. We will address this issue in following sections.

5 Chiral symmetry of staggered fermions

Let us consider the $U(1)_A$ operator Γ_ε defined in Sec. 3. Recall that an eigenmode $|f_{+\lambda}^s\rangle$ and its parity partner state $|f_{-\lambda}^s\rangle$ are related as in Eq. (5). Hence, we find that

$$\Gamma_\varepsilon |f_{+\lambda}^s\rangle = e^{+i\theta} |f_{-\lambda}^s\rangle, \quad (12)$$

$$\Gamma_\varepsilon |f_{-\lambda}^s\rangle = e^{-i\theta} |f_{+\lambda}^s\rangle. \quad (13)$$

Here, there is no constraint on the phase θ . Hence, we expect it would be real and random.

In Fig. 3, we present the probability distribution of θ for both zero modes and non-zero modes. We find that the phase θ is random in both cases.

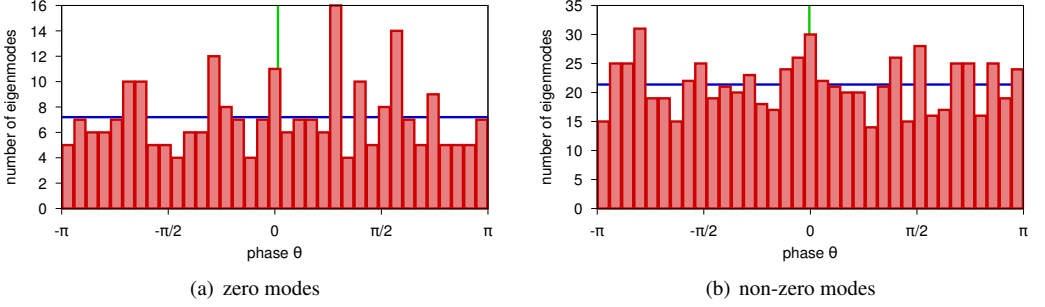


Figure 3: Histograms of the phase for the Ward identity Eqs. (12) and (13)

Let us define the chirality Γ_5 as

$$\Gamma_5(\alpha, \beta) \equiv \langle f_\alpha^s | [\gamma_5 \otimes \mathbb{1}] | f_\beta^s \rangle, \quad (14)$$

where α and β represent eigenvalues of D_s . We find that the lattice chirality operator $[\gamma_5 \otimes \mathbb{1}]$ satisfies the same recursion relations as the continuum chirality operator γ_5 :

$$[\gamma_5 \otimes \mathbb{1}]^{2n+1} = [\gamma_5 \otimes \mathbb{1}], \quad (15)$$

$$[\gamma_5 \otimes \mathbb{1}]^{2n} = [\mathbb{1} \otimes \mathbb{1}], \quad (16)$$

$$\left[\frac{1}{2}(1 \pm \gamma_5) \otimes \mathbb{1} \right]^n = \left[\frac{1}{2}(1 \pm \gamma_5) \otimes \mathbb{1} \right], \quad (17)$$

$$\left[\frac{1}{2}(1 + \gamma_5) \otimes \mathbb{1} \right] \left[\frac{1}{2}(1 - \gamma_5) \otimes \mathbb{1} \right] = 0, \quad (18)$$

where $n \geq 0$ and $n \in \mathbb{Z}$. For more details on the rigorous proof, refer to Ref. [26].

In Fig. 4, we present results for the diagonal chirality $\Gamma_5(\alpha, \alpha)$ for configurations with topological charge $Q = 0, -1, -2, -3$. In the continuum, the diagonal chirality should be ± 1 for zero modes and 0 for non-zero modes. On the lattice, the chiral symmetry for $[\gamma_5 \otimes \mathbb{1}]$ transformation is not conserved, and so the chirality operator receives renormalization. This causes the diagonal chirality to be around 0.7 instead of 1. As one can see, the diagonal chirality measurement tells us how many zero modes exist in a given configuration [2–4]. Hence, the diagonal chirality serves as a good criterion to distinguish the zero modes from non-zero modes.

6 Chiral Ward identity

Let us consider the *shift operator* which is defined as:

$$\Xi_5(\alpha, \beta) \equiv \langle f_\alpha^s | [1 \otimes \xi_5] | f_\beta^s \rangle. \quad (19)$$

Similar to the chirality operator $[\gamma_5 \otimes \mathbb{1}]$, the shift operator satisfies the following recursion relations:

$$[1 \otimes \xi_5]^{2n+1} = [1 \otimes \xi_5], \quad (20)$$

$$[1 \otimes \xi_5]^{2n} = [1 \otimes \mathbb{1}], \quad (21)$$

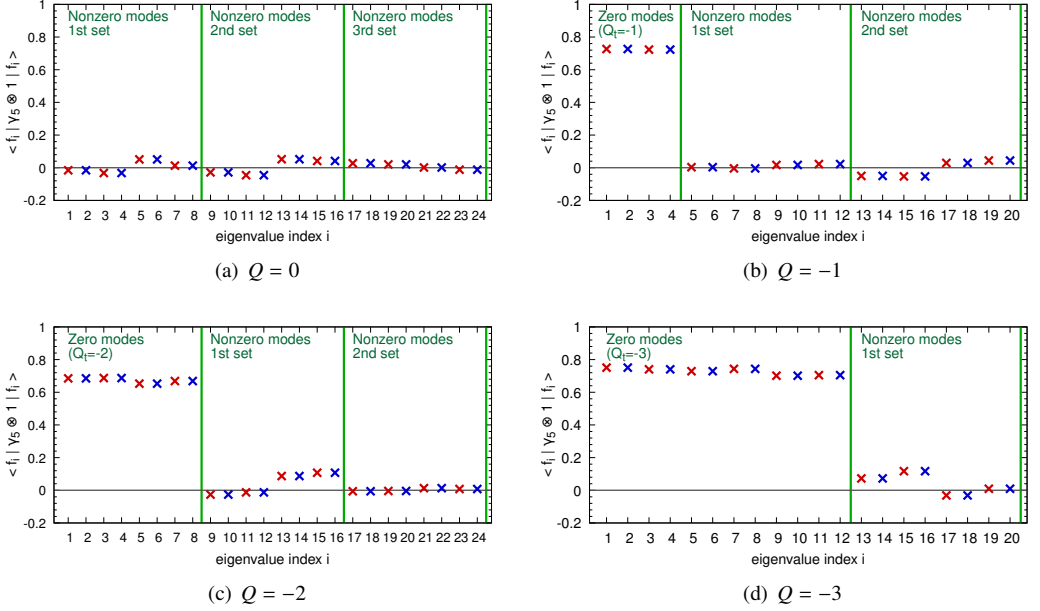


Figure 4: The chirality measurement of $\Gamma_5(\alpha, \alpha) = \langle f_\alpha^s | [\gamma_5 \otimes 1] | f_\alpha^s \rangle$ for configurations with various topological charge Q .

for $n \geq 0$ and $n \in \mathbb{Z}$.

Using Eqs. (15), (16), (20), and (21), one can find that the following relations hold:

$$\Gamma_\varepsilon [\gamma_5 \otimes 1] = [\gamma_5 \otimes 1] \Gamma_\varepsilon = [1 \otimes \xi_5], \quad (22)$$

$$\Gamma_\varepsilon [1 \otimes \xi_5] = [1 \otimes \xi_5] \Gamma_\varepsilon = [\gamma_5 \otimes 1]. \quad (23)$$

Applying them to eigenstates $|f_{\pm\lambda}^s\rangle$,

$$e^{+i\theta} [\gamma_5 \otimes 1] |f_{-\lambda}^s\rangle = [1 \otimes \xi_5] |f_{+\lambda}^s\rangle, \quad (24)$$

$$e^{-i\theta} [\gamma_5 \otimes 1] |f_{+\lambda}^s\rangle = [1 \otimes \xi_5] |f_{-\lambda}^s\rangle. \quad (25)$$

Eqs. (24) and (25) are Ward identities for the chirality of staggered fermions. We can go further. Multiplying $\langle f_{\pm\alpha}^s |$ to the left and replacing the notation λ to β , we have

$$e^{+i\theta} \Gamma_5(\pm\alpha, -\beta) = \Xi_5(\pm\alpha, +\beta), \quad (26)$$

$$e^{-i\theta} \Gamma_5(\pm\alpha, +\beta) = \Xi_5(\pm\alpha, -\beta). \quad (27)$$

Hence, we obtain the following simple Ward identities:

$$|\Gamma_5(\alpha, \beta)| = |\Xi_5(-\alpha, \beta)| = |\Xi_5(\alpha, -\beta)| = |\Gamma_5(-\alpha, -\beta)|. \quad (28)$$

In addition, the Hermiticity provides additional Ward identities:

$$|\Gamma_5(\alpha, \beta)| = |\Gamma_5(\beta, \alpha)|, \quad (29)$$

$$|\Xi_5(\alpha, \beta)| = |\Xi_5(\beta, \alpha)|. \quad (30)$$

Then, we obtain the final form of the chiral Ward identity:

$$\begin{aligned}
|\Gamma_5(\alpha, \beta)| &= |\Xi_5(-\alpha, \beta)| = |\Xi_5(\alpha, -\beta)| = |\Gamma_5(-\alpha, -\beta)| \\
&= |\Gamma_5(\beta, \alpha)| = |\Xi_5(-\beta, \alpha)| = |\Xi_5(\beta, -\alpha)| = |\Gamma_5(-\beta, -\alpha)|.
\end{aligned}
\tag{31}$$

Table 2: Numerical examples for the chiral Ward identity (WI). Here, we use the notation of $\lambda_{2n} = -\lambda_{2n-1}$ for $n \geq 1$ and $n \in \mathbb{Z}$: for example, $\lambda_{12} = -\lambda_{11}$, and $\lambda_6 = -\lambda_5$.

parameter	value	parameter	value	parameter	value
$ \Gamma_5(\lambda_1, \lambda_1) $	0.7268534	$ \Gamma_5(\lambda_5, \lambda_{12}) $	0.5903165	$ \Gamma_5(\lambda_{12}, \lambda_5) $	0.5903165
$ \Xi_5(\lambda_2, \lambda_1) $	0.7268534	$ \Xi_5(\lambda_{11}, \lambda_5) $	0.5903165	$ \Xi_5(\lambda_5, \lambda_{11}) $	0.5903165
$ \Xi_5(\lambda_1, \lambda_2) $	0.7268534	$ \Xi_5(\lambda_{12}, \lambda_6) $	0.5903165	$ \Xi_5(\lambda_6, \lambda_{12}) $	0.5903165
$ \Gamma_5(\lambda_2, \lambda_2) $	0.7268534	$ \Gamma_5(\lambda_{11}, \lambda_6) $	0.5903165	$ \Gamma_5(\lambda_6, \lambda_{11}) $	0.5903165

(a) Diagonal WI

(b) Off-diagonal WI

The chiral Ward identity in Eq. (31) is exemplified in Table 2. We find that the Ward identity holds valid up to our numerical precision.

7 Conclusion

Using the chirality measurement and Ward identities, it is possible to distinguish zero modes from non-zero modes reliably. We will address this issue in more details in Ref. [26].

Acknowledgement

We would like to express our sincere gratitude to Eduardo Follana for providing his code to us. We would like to express many thanks to Chulwoo Jung for providing the most updated CPS library to us. We would like to express our sincere gratitude to Jon Bailey and Stephen Sharpe for helpful discussion. The research of W. Lee is supported by the Creative Research Initiatives Program (No. 2017013332) of the NRF grant funded by the Korean government (MEST). W. Lee would like to acknowledge the support from the KISTI supercomputing center through the strategic support program for the supercomputing application research (No. KSC-2015-G2-002). Computations were carried out in part on the DAVID clusters at Seoul National University.

References

- [1] J. Smit, J.C. Vink, Nucl. Phys. **B286**, 485 (1987)
- [2] E. Follana, A. Hart, C.T.H. Davies, Nucl. Phys. Proc. Suppl. **153**, 106 (2006), [106(2006)]
- [3] E. Follana, A. Hart, C.T.H. Davies (HPQCD, UKQCD), Phys. Rev. Lett. **93**, 241601 (2004), hep-lat/0406010
- [4] E. Follana, A. Hart, C.T.H. Davies, Q. Mason (HPQCD, UKQCD), Phys. Rev. **D72**, 054501 (2005), hep-lat/0507011
- [5] S. Durr, C. Hoelbling, U. Wenger, Phys. Rev. **D70**, 094502 (2004), hep-lat/0406027
- [6] G.C. Donald, C.T.H. Davies, E. Follana, A.S. Kronfeld, Phys. Rev. **D84**, 054504 (2011), 1106.2412

- [7] N.D. Cundy, H. Jeong, W. Lee, PoS **LATTICE2015**, 066 (2016)
- [8] W.J. Lee, Phys. Rev. **D64**, 054505 (2001), hep-lat/**0106005**
- [9] A. Hasenfratz, F. Knechtli, Phys. Rev. **D64**, 034504 (2001), hep-lat/**0103029**
- [10] W.j. Lee, S.R. Sharpe, Phys. Rev. **D66**, 114501 (2002), hep-lat/**0208018**
- [11] W.j. Lee, Phys. Rev. **D66**, 114504 (2002), hep-lat/**0208032**
- [12] K. Orginos, D. Toussaint, R.L. Sugar (MILC), Phys. Rev. **D60**, 054503 (1999), hep-lat/**9903032**
- [13] G.P. Lepage, Phys. Rev. **D59**, 074502 (1999), hep-lat/**9809157**
- [14] A. Bazavov et al. (MILC), Rev. Mod. Phys. **82**, 1349 (2010), **0903.3598**
- [15] E. Follana, Q. Mason, C. Davies, K. Hornbostel, G.P. Lepage, J. Shigemitsu, H. Trotter, K. Wong (HPQCD, UKQCD), Phys. Rev. **D75**, 054502 (2007), hep-lat/**0610092**
- [16] T.A. DeGrand, P. Rossi, Comput. Phys. Commun. **60**, 211 (1990)
- [17] C. Lanczos, J. Res. Natl. Bur. Stand. B Math. Sci. **45**, 255 (1950)
- [18] R. Lehoucq, D.C. Sorensen, SIAM J. Matrix Anal. Appl **17**, 789 (1996)
- [19] Y. Saad, Math. Comp. **42**, 567 (1984)
- [20] M. Luscher, P. Weisz, Commun. Math. Phys. **97**, 59 (1985), [Erratum: Commun. Math. Phys.**98**,433(1985)]
- [21] M. Luscher, P. Weisz, Phys. Lett. **158B**, 250 (1985)
- [22] M.G. Alford, W. Dimm, G.P. Lepage, G. Hockney, P.B. Mackenzie, Phys. Lett. **B361**, 87 (1995), hep-lat/**9507010**
- [23] J. Kim, W. Lee, S.R. Sharpe, Phys. Rev. **D81**, 114503 (2010), **1004.4039**
- [24] J. Kim, W. Lee, S.R. Sharpe, Phys. Rev. **D83**, 094503 (2011), **1102.1774**
- [25] M. Albanese et al. (APE), Phys. Lett. **B192**, 163 (1987)
- [26] H. Jeong, W. Lee et al. (2017), in preparation